CHEMISTRY OF MATERIALS

ARTICLE

pubs.acs.org/cm

Silicate Glasses at the Ionic Limit: Alkaline-Earth Sub-Orthosilicates

N. K. Nasikas,[†,‡] A. Chrissanthopoulos,[§] N. Bouropoulos,[†,‡] S. Sen,[*,⊥] and G.N. Papatheodorou[*,†]

[†]Institute of Chemical Engineering and High Temperature Chemical Processes, Foundation for Research & Technoloy−Hellas (FORTH), P.O.Box 1414, GR-26504, Patras, Greece

[‡]Departmentof Materials Science and [§]Department of Chemistry, University of Patras, GR-26504, Patras, Greece

[⊥]Department of Chemical Engineering & Materials Science, University of California at Davis, Davis, California 95616, United States

Supporting Information

ABSTRACT: Container-less levitation techniques and CO_2 laser heating were used to prepare a series of silicate glasses along the compositional join $(1-x)(Ca,Mg)O-xSiO_2$ beyond the orthosilicate limit for the first time with the silica mole fraction x ranging between 0.33 and 0.27. Raman spectroscopic measurements in the temperature range 25−700 °C show complete absence of connectivity between the SiO_4 tetrahedra in glasses with $x < 0.3$. The corresponding glass structures are characterized by isolated negatively charged "tetrahedral" SiO_4^{4-} and O^{2-} anions with M^{2+} (M = Mg,Ca) as the counter cations, held together by pure Coulombic (ionic) interactions. This structural view is supported by semiempirical MO simulations which were used to derive the structure of the Ca,Mg suborthosilicate glass $0.5(1-x)CaO-0.5(1-x)MgO-xSiO_2$ with $x = 0.286$. The Raman spectra permit the experimental determination of all the vibrational modes of the isolated SiO_4^{4-} tetrahedra in silicate glasses.

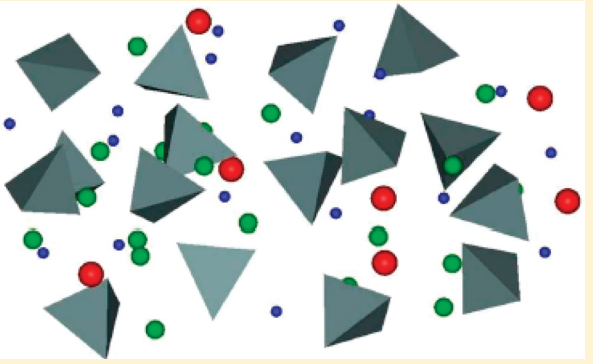

KEYWORDS: sub-orthosilicates, glass formation, Raman spectroscopy, ionic limit

INTRODUCTION

Silicate glasses are important technological materials that have found widespread use in our lives. Crystalline and glassy silicates are the most important constituents of the terrestrial and lunar crust and mantle and meteorites.[1] The structure of crystalline and glassy silica consists of a network of SiO_4 tetrahedra corner-sharing via bridging oxygens (BO). The connectivity of this network is disrupted on addition of alkali and/or alkaline-earth cations with the creation of non-bridging oxygens (NBO) and the silicate glass structure is thus described in terms of Q^i species where $4 \geq i \geq 0$ denotes the number of bridging oxygens on the SiO_4 tetrahedra that form Si−O−Si linkages in the network.[2] Extreme depolymerization is obtained in nature in crystalline orthosilicates with 33.33 mol % SiO_2 where the crystal structure is composed of isolated $(SiO_4)^{4-}$ tetrahedra, i.e., Q^0 species.[2] It is generally believed that the lack of network formation via Si−O−Si bonding in such compositions constitute the limit of glass formation for all oxide liquids in general.[3] An example is the composition Mg_2SiO_4 (forsterite) that is extremely difficult to vitrify even with the use of containerless levitation techniques and CO_2 laser heating.[4,5] The structure of forsterite glass has been extensively investigated with Raman[4] and nuclear magnetic resonance (NMR)[5] spectroscopy as well as with X-ray and neutron scattering methods.[3,6] It is evident from these works that even in the extreme case of the forsterite glass only ∼50% of the Q^i species are the "free" SiO_4^{4-} (Q^0) species with the other 50% being mainly the dimeric Q^1 (i.e., $[Si_2O_7]^{6-}$) species.[4,5] The formation of Q^1 species in the Mg_2SiO_4 glass implies that "free" oxygen ions are released from Q-species disproportionation reactions that can be written as: $2Q^0 = 2Q^1 + O^{2-}$. The disproportionation reaction is increasingly driven to the right with increasing field strength i.e. charge:radius ratio of the modifying cation. These "free" oxygen ions are expected to be charge balanced by and bonded to Mg^{2+} ions in the structure, as is indeed observed in the high-pressure polymorph of the mineral forsterite (Mg_2SiO_4), known as wadsleyite.[5] It has been suggested by Kohara et al. on the basis of diffraction studies that the stabilization of the Mg_2SiO_4 glass is related to the formation of a percolation domain of interconnected MgO_x (x = 4,5,6) polyhedra where 4 and 5 coordinated Mg sites dominate the structure.[3] On the other hand, our previous structural studies based on Raman, ^{29}Si and ^{25} Mg NMR spectroscopy suggested that the invert Mg-silicate glasses with ≥60 mol % MgO can be stabilized by the formation of a network of interconnected SiO_4 and MgO_6 polyhedra where the SiO_4 tetrahedra are present as Q^0 and Q^1 species. Although it is still not clear exactly what structural aspects are responsible for glass formation in a nominally orthosilicate composition, the presence of multiple types of

Received: May 3, 2011
Revised: July 12, 2011
Published: July 26, 2011

Q-species in Mg_2SiO_4 glass may be partly responsible for an entropic stabilization of the vitreous form upon rapid cooling.

Previous calorimetric studies have shown that the presence of multiple types of network modifying cations (e.g., Ca and Mg) can substantially contribute to the configurational entropy of a liquid and thereby may give rise to an increase in its fragility compared to a liquid with a single type of modifier cation.[7] Typically fragile liquids are worse glass-formers than strong liquids and hence it would be expected that simple silicate liquids with single modifying cation would vitrify more easily compared to a liquid with the same silica content but with mixed modifiers. On the other hand, multiple types of network modifiers in an oxide liquid can be characterized by their distinct bonding environments and oxygen coordination polyhedra. This can enhance the glass-forming ability of the liquid by increasing its structural and topological frustration and thereby not allowing the liquid to find the global minimum in its potential energy landscape which corresponds to the crystal structure. Such entropic and topological effects are expected to be maximized near a 1:1 ratio of the modifiers in a system with two different modifying cations. The topological frustration hypothesis has provided us with the motivation to attempt the vitrification of suborthosilicate compositions in the pseudobinary system $(1-x)(Ca,Mg)O-xSiO_2$ with $x < 0.33$.

In this study, we have used containerless aerodynamic levitation techniques and CO_2 laser heating[8,9] to synthesize suborthosilicate glasses of the type $(1-x)(Ca,Mg)O-xSiO_2$ with $0.27 \leq x \leq 0.33$ and CaO:MgO = 1:1. The glass compositions prepared in this study with $x = 0.333$, 0.32, 0.30, 0.28, and 0.27 are denoted in the subsequent discussion as CMS33.3, CMS32, CMS30, CMS28, and CMS27, respectively. The structures of these glasses have been investigated using Raman spectroscopy and quantum mechanical calculations based on semiempirical Molecular Orbital theory.

EXPERIMENTAL SECTION

Synthesis. The starting chemicals for syntheses of these glasses were regent grade SiO_2 (99.999% pure, Puratronic powder), MgO (99.95% pure, powder) and CaO (99.95% pure, powder), all purchased from Alfa Aesar. The oxides were dried in a furnace at ~400 °C for 24 h and were batched to prepare compositions $(1-x)(Ca,Mg)O-xSiO_2$ with $x = 0.333$, 0.32, 0.30, 0.28, and 0.27. The vitrification of these oxide mixtures was achieved by CO_2 laser melting and the aerodynamic levitation methods which has been described in detail elsewhere.[4,8,9] The final step of the synthesis involved heating and melting of the levitated samples followed by rapid quenching via sudden shutdown of the CO_2 laser that yielded spherical, completely colorless and transparent amorphous beads of about 1−1.5 mm in diameter. The factors influencing the success in vitrifying the liquid droplets were the uniformity of temperature and the size of the levitated liquid sphere as well as the rate of quenching. We had no easy way to control all these factors so the preparations were mainly a "trial and error" process. The success rate for these "trial and error" experiments decreased with decreasing silica content for the CMS28 and CMS27 the success rate was less than 10%. No glasses could be obtained with silica mole fractions $x < 0.27$. Chemical analyses by electron microprobe indicated that the stoichiometry of the prepared glass samples were within ±1 wt % of the nominal compositions. Finally, it should be noted that attempts to prepare the CMS33.3 glass by the sol gel methods through the hydrolysis of tetraethylorthosilicate in acid catalyst were unsuccessful.

Raman Spectroscopy. Raman spectra were measured with a versatile system described before.[9] The ~1 mm diameter spherical glass beads were placed on an $X-Y-Z$ stage and the 514.5 nm laser line of the spectrometer was focused on the sample using a 145 mm focal length (FL) lens. Laser power of 300 mW (measured on the sample) was used with the beam passing along the diameter and focused at the center of the glassy sphere, thus, minimizing light reflections and permitting measurements close to the excitation line thereby resolving the Boson peak. Stokes-side Raman spectra were recorded with a 90° scattering geometry using a collecting lens system (80 and 260 mm FL) coupled to a double monochromator (T-64000 Jobin−Yvon) and equipped with a CCD detector. The wavelength resolution of the instrument was 2 cm^{-1} and the frequencies are associated with an error $< \pm 2$ cm^{-1} for the whole set of measurements. Both scattering geometries, polarized (VV: vertical laser excitation-vertical analysis of scattered light) and depolarized (VH: vertical laser excitation-horizontal analysis of scattered light), were employed. The effect of temperature on the Raman spectra was studied for the CMS28 glass between room temperature and 700 °C. A homemade optical furnace was used for these in situ measurements of the Raman spectra at elevated temperatures.[4] The glass transition temperatures of these CMS glasses are not known but probably are below 1000 °C because Raman spectra of most of these glasses showed signs of crystallization near and above 800 °C.

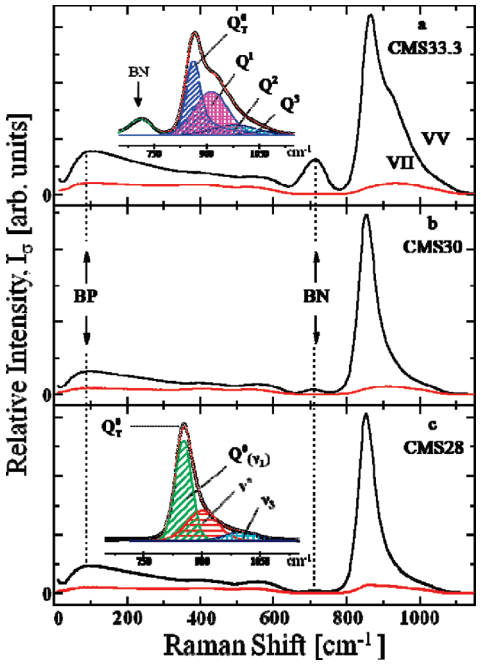

Figure 1. (a−c) Raw Stokes-side Raman spectra of the $(1-x)(Ca,Mg)O-xSiO_2$ glasses. Lower (red) and upper (black) curves denote the depolarized (VH) and polarized (VV) spectra, respectively. Spectral conditions: excitation line 514.5 nm; laser power 300mW; resolution 2 cm^{-1}; CCD detector. Spectra of the CMS32 sample had an intermediate shape between the CMS33.3 and CMS30 spectra while the CMS27 spectra were the same as the CMS28 spectra. BP and BN denote the Boson peak band and the Si−O−Si bending mode band respectively. Note that as x decreases, the BN band diminishes in intensity and is practically disappears in the CMS28 spectra which is a strong evidence for the absence of any bridged Q species in this glass. Insets in a and c show deconvolution of the high-frequency bands in the reduced VV representation. Inset in c shows the Q_T^0 band analysis of the CMS28 glass to three Gaussian bands associated with the ν_1, ν_3, and $\nu^* = 2\nu_2$ modes of the SiO_4^{4-} tetrahedra. Inset in a shows the deconvolution of the CMS33.3 glass band involving the Q_T^0 band and three bands corresponding to Q^i (i = 1, 2, and 3) species.

dx.doi.org/10.1021/cm2012582 |Chem. Mater. 2011, 23, 3692–3697

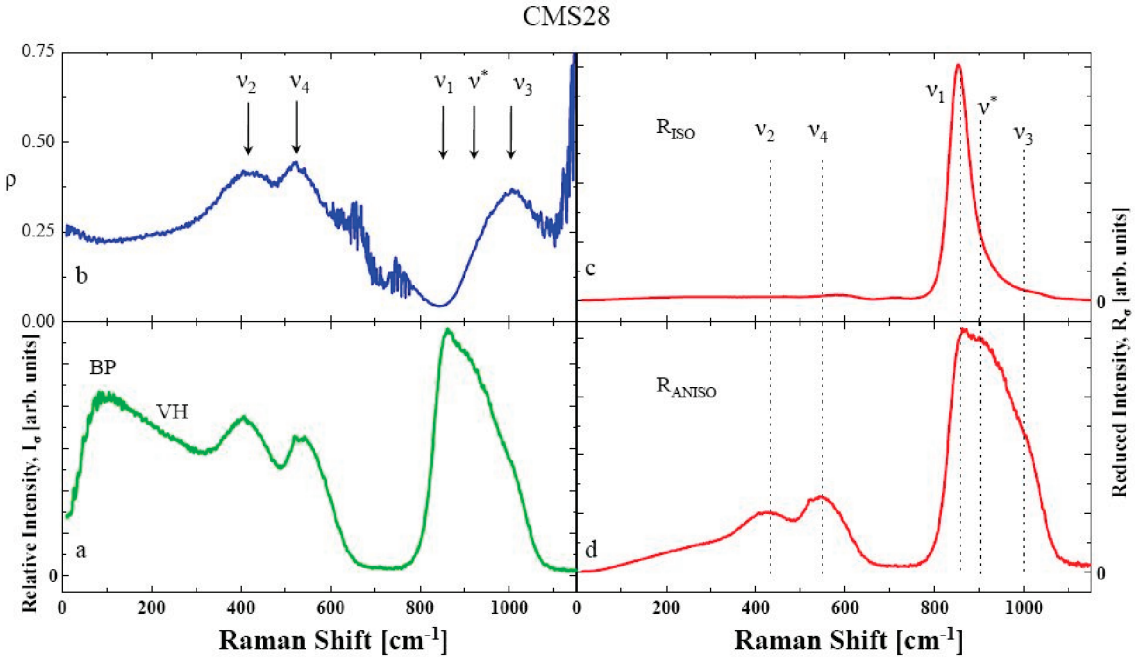

Figure 2. Details of the CMS28 Raman spectra: (a) expanded depolarized (VH) spectra, (b) linear depolarization ratio $\rho = I_{VH}/I_{VV}$; in the spectral region where the intensities I_{VV} and I_{VH} approach zero the noise in ρ increases; the maxima indicate the presence of depolarized bands in the Raman spectra. (c) Reduced isotropic (ISO = VV − (4/3)VH, see the Supporting Information[11]) spectra calculated from the raw Raman data; details for the reduction process are given in refs 4 and 11; only the polarized bands appear in this representation. (d) Reduced anisotropic (VH = ANISO) spectra calculated as in c. The vertical lines ν_1 = 853, ν_2 = 425, ν_3 = 1000, and ν_4 = 550 cm^{-1} denote the fundamental frequencies of the Q^0 tetrahedra and ν^* denotes the Fermi resonance overtone (2 ν_2, see text).

RESULTS AND DISCUSSION

Typical polarized and depolarized (VV and VH) Raman spectra of the CMS33.3, CMS30 and CMS28 compositions are shown in Figure 1. The Raman spectra of the CMS33.3 glass do not show any significant difference with respect to the corresponding spectra of the forsterite glass reported previously in the literature.[4] The high-frequency band envelope between 800 and 1100 cm^{-1} (Figure 1) covers the symmetric Si−O stretching vibrations of the Q^i ($3 \geq i \geq 0$) species with the signature for the Q^0 species at ∼860 cm^{-1} having the highest intensity. The Si−O−Si bending modes give rise to the band designated as BN centered at ∼700 cm^{-1}, whereas the band BP at ∼93 ± 2 cm^{-1} corresponds to the Boson peak.[4] Upon lowering the silica content the high frequency band envelope becomes narrower, the BN band diminishes in intensity and finally disappears for glasses with $x < 0.3$ providing the most definitive evidence for the absence of any Si−O−Si linkages in these glasses, i.e., their structure contains solely the isolated Q^0 (SiO_4^{4-} tetrahedra) species . Concomitant with the disappearance of the BN band, two new low-frequency depolarized bands appear near ∼430 and ∼550 cm^{-1}. These two bands are clearly observed in the magnified view of the VH and the reduced anisotropic[11] Raman spectra of the CMS28 glass as shown in Figure 2. The depolarization characteristics of the above-mentioned bands are better seen in the isotropic and anisotropic Raman spectra in the reduced representation[10,11] along with the spectral linear depolarization ratio ρ (Figure 2).

By combining the information given in Figure 2, five distinct bands can be recognized in the Raman spectra of the CMS28 glass besides the BP at ∼93 cm^{-1}. The SiO_4^{4-} tetrahedron (Q^0 species) with its T_d symmetry is characterized by nine normal modes of vibration with one $A_1(\nu_1)$, one doubly degenerate E (ν_2), and two triply degenerate T_2 (ν_3, ν_4) modes, all of which are Raman active. The bands at ∼430 and ∼550 cm^{-1} are present in the anisotropic spectra (Figure 2a,c) and show maxima in the depolarization ratio (Figure 2b). These bands are assigned to the ν_2 (E) and ν_4 (T_2) bending modes of the SiO_4^{4-} tetrahedra, respectively, whereas the high-intensity polarized isotropic band at ∼853 cm^{-1} represents the ν_1 (A_1) symmetric stretching mode. The shape of the ν_1 (A_1) band is asymmetric and contains contributions from two higher frequency bands at ∼900 and 1000 cm^{-1}. The weak band at ∼1000 cm^{-1} appears as a shoulder in the anisotropic spectra (Figure 2c) and has a well-defined maximum in the depolarization ratio spectra (Figure 2b). This band is likely to be associated with the ν_3 (T_2) antisymmetric stretching mode of the SiO_4^{4-} tetrahedra. The frequencies of all four bands ν_1, ν_2, ν_3, and ν_4 are completely consistent with the spectral regions where the splitting of the internal modes of the SiO_4^{4-} tetrahedra in the orthosilicate $CaMgSiO_4$ crystal monticellite have been measured.[12]

The assignment of the $\nu^* = 900$ cm^{-1} band contributing to the asymmetry of the main polarized band is not straightforward especially because this band is in the frequency range characteristic of the Q^1 species, as observed in the orthosilicate glasses.[4] However, the absence of the BN band from the VV and R_{VV} spectra of the CMS28 glass (Figures 1 and 2) excludes the possibility of the presence of Q^1 species in any significant concentration in this glass. This result suggests that the origin of the ν^* band is more likely intrinsic of the vibrations of the SiO_4^{4-} tetrahedra. The most likely assignment would be the first overtone of the ν_2(E) mode. The symmetry of the overtone $2\nu_2$ is given by the cross product $\mathbf{E} \times \mathbf{E} = \mathbf{A_1} + \mathbf{E}$, which contains an A_1

dx.doi.org/10.1021/cm2012582 |Chem. Mater. 2011, 23, 3692–3697

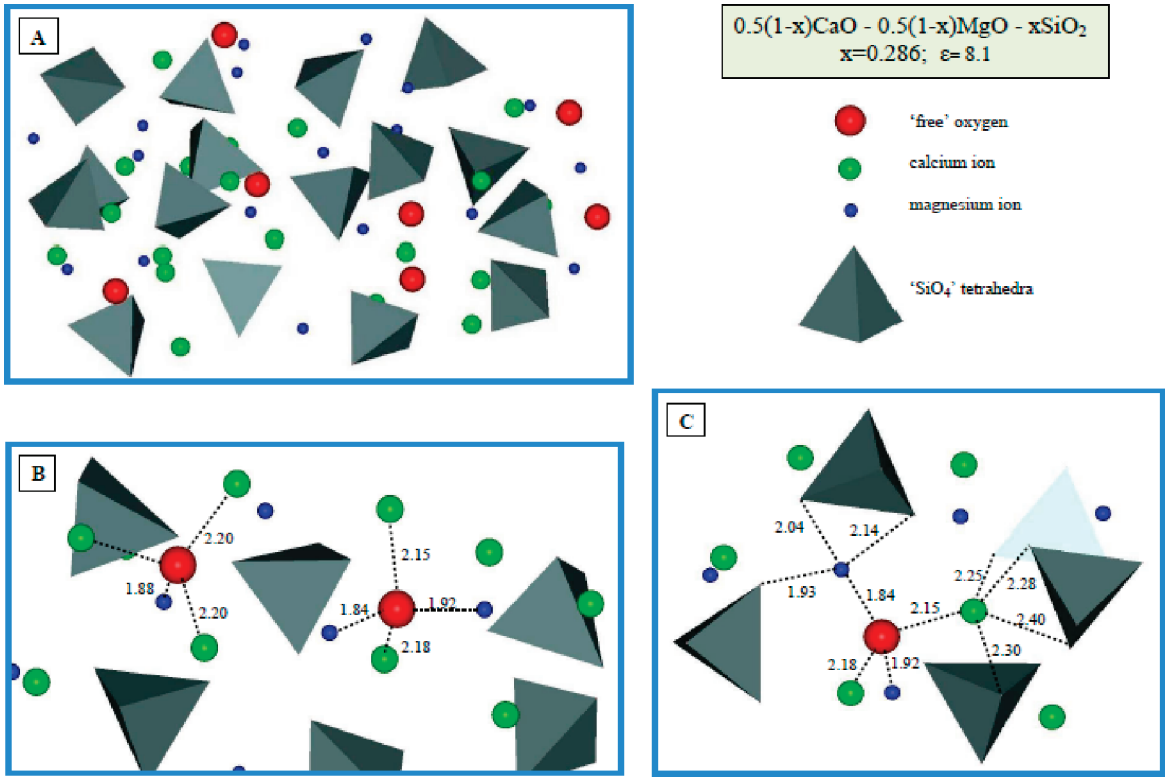

Figure 3. (A) Structural model of the 0.357MgO−0.357CaO−0.286SiO_2 bulk glass as obtained from MOPAC/PM6-D calculation representing the fully optimized geometry for a system of 128 atoms. Details for the calculations are given in the Supporting Information. (B) Typical coordination environment of the "free" oxygen anions. Four alkaline earth ions formed the first coordination sphere of the oxygen at a distance of 1.8−2.2 Å ; other cations are at distances greater than 3 Å. (C) Typical coordination environment of the alkaline earth cations bound to the corners and edges of the tetrahedra as well as to "free" oxygen anions. The coordination numbers shown here are four and five for magnesium and calcium respectively but higher coordination numbers (5 and 6) can be found in other regions. The interatomic distances are 1.80−2.15 Å for Mg−O and 2.15−2.4 Å for Ca−O.

symmetry species, and its frequency ($2\nu_2 \approx 850\ cm^{-1}$) overlaps with that of the ν_1(A) symmetric stretching mode . This is an ideal case for Fermi resonance[13] interaction between the $2\nu_2$ and ν_1 vibrational states, which implies that (a) the two states with A_1 symmetry repel each other and thus the frequency of $2\nu_2$ band splits away from that of ν_1 and (b) the otherwise weak intensity of the $2\nu_2$ overtone is enhanced dramatically and thus contributes to the asymmetry of the ν_1 band. Both requirements are fulfilled for the ν^* band and validates its assignment to the $2\nu_2$ overtone. The three-band (ν_1, ν_3, and ν^*) Gaussian deconvolution of the asymmetric high-frequency band corresponding to the intrinsic vibrations of the SiO_4^{4-} tetrahedra in the Raman spectrum of the CMS28 glass is shown in the inset of Figure 1c. This asymmetric band is denoted as Q_T^0 and is a superposition of the $A_1(\nu_1)$ band assigned to the Q^0 species plus the above-mentioned ν_3 and ν^* bands. With the use of the Q_T^0 band the high-frequency band in the Raman spectrum of the CMS33.3 glass can be deconvoluted (Figure 1a, inset) resulting in the following relative fractions (within ±3%) of the various Q-species in the glass: 50% Q^0, 35% Q^1, 13% Q^2, and 2% Q^3. Such Q-speciation for the Ca−Mg orthosilicate glass is similar to that observed for Mg_2SiO_4 glass in a previous study[4] with 49% Q^0, 31% Q^1, 14% Q^2, and 6% Q^3.

The Raman spectra of these glasses show no vibrational modes associated with any M−O vibration (M = Ca, Mg) of the MO_Z polyhedra. This is an indication of weak or absent covalent bonding within the MO_Z polyhedra and in-between neighboring M^{2+} cations. Consequently, the MO_Z polyhedra are "held" together by Coulombic forces and have shorter vibrational lifetimes relative to those of the stable SiO_4^{4-} tetrahedra, which in turn imply that these glasses are ionic in character. Finally, the stoichiometry of these glasses implies that all suborthosilicate compositions with less than 33.33 mol % SiO_2 should contain "free oxygens" i.e., O^{2-} anions bonded only to the M^{2+} cations. For example in the case of the CMS28 glass (x = 0.28) the stoichiometry corresponds to about four free oxygen for every seven Q^0 tetrahedra which translates to ∼7% of all oxygen atoms being bonded only to the M^{2+} cations. Unequivocal detection of such small amount of free oxygen in the structure would require the application of ^{17}O NMR spectroscopy on isotopically enriched samples. Such studies are currently underway in our laboratories.

When taken together the Raman spectroscopic results indicate that the CMS28 glass is composed of SiO_4^{4-} anions with Mg^{2+} and Ca^{2+} as the counter cations. The strong Coulombic forces require that each SiO_4^{4-} anion is surrounded by cations and vice versa. This structural picture is indeed borne out in our simulation of the structure of a glass of composition CMS28.6 (x = 0.2857) glass (Figure 3), corresponding to the mixture 20MgO−20CaO−16SiO_2 using semiempirical molecular orbital theory (see the Supporting Information for details[11]). The simulated structure shows that in these alkaline-earth rich suborthosilicate glasses the anionic SiO_4^{4-} tetrahedra are held together by the Mg^{2+} and Ca^{2+} counter-cations whose preferential coordination is retained by the flexible orientation of the terminal oxygens of the SiO_4^{4-} tetrahedra plus the available free oxygens (Figure 3).

dx.doi.org/10.1021/cm2012582 |*Chem. Mater.* 2011, 23, 3692–3697

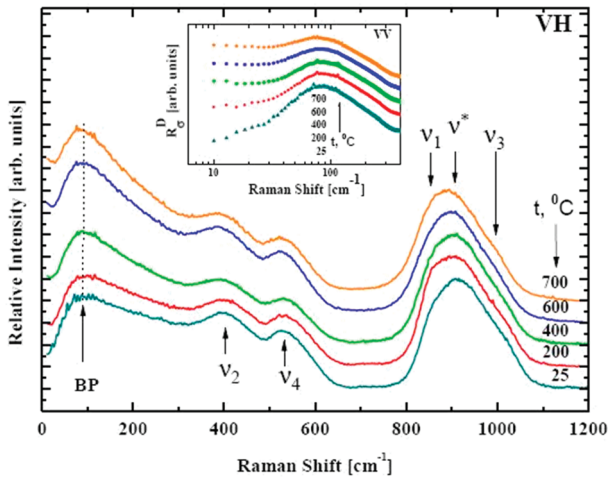

Figure 4. Raw depolarized (VH) Raman spectra of the CMS28 glass at temperatures ranging between ambient and 700 °C. Inset: Frequency-reduced Boson peak (R^D_σ) in logarithmic frequency scale. The spectra were calculated from the reduced R_σ (σ = VV or VH) data and the relation $R^D_\sigma = R_\sigma \nu^{-2}$ (see the Supporting Information[11]) and can be directly compared with the R^D_σ spectra of the forsterite glass.[4] For both systems, there is practically no shift of the BP frequency with temperature.

This structural scenario is reminiscent of that of the highly fragile alkali and alkaline-earth nitrate ionic glasses where randomly oriented nitrate (NO_3^-) anions are held together by their Coulombic interaction with the alkali and alkaline-earth cations.[14]

Figure 4 shows the temperature dependence of depolarized VH Raman spectra of the CMS28 glass. Similar spectra were also measured in the VV configuration but because of the high band intensity in the stretching mode region (800−1100 cm^{-1}), the effects of temperature on the bending modes do not show up as prominently as in the VH spectra (see Figure 1). The vibrational bands become broader with increasing temperature and in the VH (or VV) representation of the spectra appear to exhibit red shifts in frequency. However, once the effects of temperature on the frequency and asymmetry of the low energy ν_2 and ν_4 bands are corrected, no temperature-dependent frequency shifts are observed for these bands in the reduced representation of the spectra. On the other hand, the ν_1 streching mode, which is coupled with Fermi resonance (ν^*) shifts to lower frequency with increasing temperature (see the Supporting Information). Such red shifts in the frequencies of the stretching modes have been observed previously in temperature dependent Raman spectroscopic studies of inorganic crystals and melts[10] and are attributed to the weakening of the central atom−ligand bonding due to volume expansion. Thus the vibrational amplitudes of the Q^0 tetrahedra in the CMS28 glass increase with temperature and the Si−O intratetrahedral bonding is weakened resulting in a broadening of the ν_1 Raman band with concomitant shift to lower frequencies.

In the low-frequency region of the Raman spectra the BP intensity of all glasses studied (Figure 1) decreases monotonically with decreasing silica content without any significant change in its frequency. The diminishing intensity, without frequency softening, may imply that the excess vibrational density of states (VDoS) in the glass that give rise to the BP is lowered as the structure becomes more ionic and the VDoS approaches that of the crystalline solid. With increasing temperature from 25 to 700 °C the relative intensity of the BP in the CMS28 Raman spectra (Figure 4) increases following the Bose-Einstein statistics[10,11] and its frequency shifts slightly to lower energies (Figure 4 inset). This behavior is similar to that observed in glasses along the Mg_2SiO_4−$MgSiO_3$ pseudobinary join where the BP frequency at ∼95 ± 3 cm^{-1} is practically invariant of composition and of temperature below glass-transition.[4] This result is in sharp contrast with that observed in almost all inorganic glasses (except in pure silica) where the BP frequency decreases upon heating and exhibits frequency shifts that depend on the concentration of the network modifier alkali and/or alkaline earth oxides.[15]

A number of previous studies in the literature have suggested a purely empirical correlation between BP intensity of glasses and the fragility of the corresponding parent liquids.[15,16] This empirical correlation is based on the observation that the BP intensity in glasses derived from fragile liquids are typically lower than that in glasses derived from strong liquids. It should be noted here that the fundamental origin of such a correlation is still not known and recent studies have indicated that existing models and interpretations of such purely empirical correlations are problematic and unsuccessful to provide a universal picture that agrees with all available experimental facts.[10,17−19] Keeping this caveat in mind and assuming that such a correlation might be valid for glasses that belong to a single compositional series then the observed monotonic drop in the BP intensity with decreasing silica content in the CMS glasses studied here can be interpreted to indicate a corresponding increase in the fragility. A comparison of the normalized BP intensity of the CMS33.3 orthosilicate glass with that of the Mg_2SiO_4 glass whose Raman spectrum was published in a previous study[4] indicates that the former is nearly 30% lower than the latter. This result is consistent with the hypothesis that the CMS33.3 liquid is expected to be more fragile than the Mg_2SiO_4 liquid due to the presence of multiple types of network modifying cations (i.e., Ca and Mg) in the former that can substantially contribute to its configurational entropy. As mentioned before, the Q-speciation of these two glasses are nearly identical. Therefore, when both the structure and the fragility of CMS33.3 and Mg_2SiO_4 liquids are taken into consideration it is clear that the higher glass-forming ability of the former liquid cannot be explained on the basis of either of these characteristics. Rather it appears that the above-mentioned topological frustration model for the packing of the modifier-oxygen coordination polyhedra can explain the better glass-forming ability of the mixed-modifier CMS33.3 composition compared to that of Mg_2SiO_4.

Finally, it should be noted that the suborthosilicate CMS compositions studied here are not expected to be glass-formers according to our conventional wisdom and furthermore their extreme ionic character have been practically unknown to date in silicate liquids. Therefore, future studies of these novel materials can have a major impact in our current understanding of glass structure and liquid-to-glass transition in oxide networks. Moreover, such liquids and glasses are expected to possess unusual properties such as high fragility index,[20] strong bioactivity[21] and high solubility of rare earth ions[22] and therefore may find potential applications in biomedical implants and in photonics as host materials for lasers and optical amplifiers.

SUMMARY

Alkaline earth suborthosilicate glasses with SiO_2 contents ranging between 33.3 and 27 mol % are prepared by container-less

levitation techniques combined with CO_2 laser heating and melting. Raman spectroscopic measurements indicate that the structure of these glasses consists of a "network" held together by pure Coulombic (ionic) interactions between the isolated SiO_4^{4-} tetrahedra, the free oxygens and the alkaline earth cations. The free oxygens present distribute their charge between the alkaline earth cations M^{2+} whose preferential coordination environment is attained by the flexible orientation of the SiO_4^{4-} tetrahedra sharing their terminal oxygens with the central cation. This structural view is also supported by semiempirical MO simulations which show the local environment around the stabilized SiO_4^{4-} anions, as well as the interatomic distances between SiO_4^{4-} and Ca^{2+}, Mg^{2+}, and O^{2-} ions. The present work shows that glass formation is possible even beyond the orthosilicate composition, which was believed to constitute the limit of silicate glass formation. Finally analysis of the Raman spectra resolved for the first time all the fundamental frequencies of the vibrational modes of isolated SiO_4^{4-} tetrahedra in the glassy state.

■ ASSOCIATED CONTENT

Supporting Information. Computational details and additional figures (PDF). This material is available free of charge via the Internet at http://pubs.acs.org/.

■ AUTHOR INFORMATION

Corresponding Author

*E-mail: sbsen@ucdavis.edu (S.S.); gpap@iceht.forth.gr (G.N.P.).

■ ACKNOWLEDGMENT

The financial support to N.K.N. and G.N.P. from the Executive Board of FORTH is acknowledged. S.S. was supported by the National Science Foundation grant DMR0906070.

■ REFERENCES

(1) Stixrude, L.; Karki, B. *Science* **2005**, *310*, 297.
(2) Mysen, B.; Richet, P. In *Silicate Glasses and Melts: Properties and Structure*; Elsevier B.V.: Amsterdam, 2005.
(3) Kohara, S.; Suzuya, K.; Takeuchi, K.; Loong, C.-K.; Grimsditch, M.; Weber, J. K. R.; Tangeman, J. A.; Key, T. S. *Science* **2004**, *303*, 1649.
(4) Kalampounias, A. G.; Nasikas, N. K.; Papatheodorou, G. N. *J. Chem. Phys.* **2009**, *131*, 114513 and references therein.
(5) Sen, S.; Maekawa, H.; Papatheodorou, G. N. *J. Phys. Chem.* **2009**, *113*, 15243and references therein.
(6) Wilding, M. C.; Benmore, C. J.; Weber, J. K. R. *J. Mater. Sci.* **2008**, *43*, 4707.
(7) Richet, P. *Geochim. Cosmochim. Acta* **1984**, *48*, 471.
(8) Kalampounias, A. G.; Papatheodorou, G. N. In *13th International Symposium on Molten Salts*, PV 02−19; Trulove, P. C., De Long, H. C., Mantz, R. A., Stafford, G. R., Matsunago, M., Eds.; The Electrochemical Society Proceedings Series; The Electrochemical Society: Pennington, NJ, 2002; p 485.
(9) Papatheodorou, G. N.; Kalampounias, A. G.; Yannopoulos, S. N. In *Molten Salts and Ionic Liquids: Never the Twain?*; Gaune-Escard, M., Seddon, K. R., Eds.; John Wiley & Sons: New York, 2009.
(10) Papatheodorou, G. N.; Yannopoulos, S. N. In *Molten Salts: From Fundamentals to Applications*; Gaune-Escard, M., Ed.; Kluwer Academic Publishers:Dordrecht, The Netherlands, 2002; p 47.
(11) Computational details and other Supporting Information are available online.
(12) Handi, M.; Kosinski, K.; Tarte, P. *J. Mol. Struct.* **1985**, *115*, 401.
(13) Fermi, E. *Z. Phys.* **1931**, *71*, 250.
(14) Angell, C. A. *Science* **1995**, *267*, 1924.
(15) Angell, C. A. *J. Non-Cryst. Solids* **1991**, *131*−*133*, 15.
(16) Sokolov, A. P.; Rossler, E.; Kisliuk, A.; Quitmann, D. *Phys. Rev. Lett.* **1993**, *71*, 2062.
(17) Yannopoulos, S. N.; Papatheodorou, G. N. *Phys. Rev. B* **2000**, *62*, 3728.
(18) Yannopoulos, S. N.; Andrikopoulos, K. S.; Ruocco, G. *J. Non-Cryst. Solids* **2006**, *352*, 45.
(19) Kalampounias, A. G.; Yannopoulos, S. N.; Papatheodorou, G. N. *J. Non-Cryst. Solids* **2006**, *352*, 4619.
(20) Angell, C. A.; Ngai, K. L.; McKenna, G. B.; McMillan, P. F.; Martin, S. W. *J. Appl. Phys.* **2000**, *88*, 3113.
(21) Oliveira, J. M.; Correia, R.; Fernandes, M. H. *Biomaterials* **2002**, *23*, 371.
(22) Beall, G. H.; Pinckney, L. R. U.S. Patent 6531420B1, 2003.